Supporting Information

Supporting Methods

Mean-squared displacement

For two-dimensional Brownian motion, the diffusion coefficient, *D*, of a molecule is proportional to the slope of its mean-squared displacement (MSD, $\langle r^2 \rangle$) curve:

$$\langle r^2 \rangle = 4D\tau \tag{S1}$$

where τ is the time lag, i.e., the amount of time in which the displacements occur (Qian *et al.*, 1991).

Cumulative probability distributions

For homogeneous two-dimensional Brownian motion, the probability of a molecule remaining within a circle of radius, *r*, in a time lag, τ, is:

$$P(r^2, \tau) = 1 - \exp\left(\frac{-r^2}{\langle r^2 \rangle + \sigma^2}\right) \tag{S2}$$

where σ is the 30 nm localization accuracy (Sonnleitner *et al.*, 1999; Lommerse *et al.*, 2004; van den Wildenberg *et al.*, 2011). To permit heterogeneous motion, multiple populations with unique MSD values are incorporated by including additional exponential terms in the expression. Based on goodness of fit to our data, we use a three-term model: two mobile terms with weights α and β, respectively, and one immobile term (i.e. $\langle r_\gamma^2 \rangle = 0$) with weight $\gamma = 1 - (\alpha + \beta)$:

$$P(r^2, \tau) = 1 - \alpha \cdot \exp\left(\frac{-r^2}{\langle r_\alpha^2 \rangle + \sigma^2}\right) - \beta \cdot \exp\left(\frac{-r^2}{\langle r_\beta^2 \rangle + \sigma^2}\right) - \gamma \cdot \exp\left(\frac{-r^2}{\sigma^2}\right) \tag{S3}$$

Bootstrap error analysis

Displacement data for each of the three cell strains at each time lag were resampled with replacement 1000 times. Each sample was equal in size to the original dataset from which it was taken, e.g. 21057 50-ms displacements were chosen from the TcpP-PAmCherry dataset (Table 2). The CPD was calculated and fit with the three-term model above (Eq. S3) for each sample. The mean values and standard deviations of the resulting fit parameters (i.e. α, β, γ, $\langle r_\alpha^2 \rangle$, and $\langle r_\beta^2 \rangle$) are reported in Table 3.

Monte Carlo simulations

Simulations were performed in MATLAB. The cell membrane was modeled as the surface of a half-cylinder 2 μm long and 0.6 μm in diameter, to match the dimensions of a *V. cholerae* bacterium (Kay *et al.*, 1994). Each of 200 molecules was allowed to diffuse on this surface for 20 frames, starting at a random position. Displacements were chosen from a normal distribution corresponding to a diffusion coefficient of 0.066 $\mu m^2/s$. The three-dimensional molecular positions at each frame were then projected onto a plane parallel to the cell. CPD analysis of these projected displacements revealed an apparent immobile population of 2–6%.

Supporting Figures

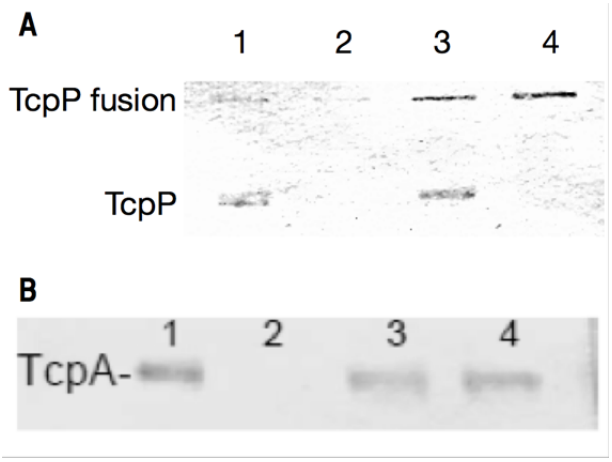

Fig. S1. Stability and activity of the TcpP-PAmCherry fusion protein

Expression of TcpP/TcpP fusions (A) and of *toxT*-activated TcpA (B) were determined by immunoblotting. The following strains were used: O395 (wild type; lane 1), Δ*tcpP* (lane 2), Δ*tcpP* TcpP-mCherry (lane 3), and Δ*tcpP* TcpP-PAmCherry (lane 4). Due to the observed instability of the TcpP-mCherry fusion protein, only the TcpP-PAmCherry fusion was used for microscopic analysis.

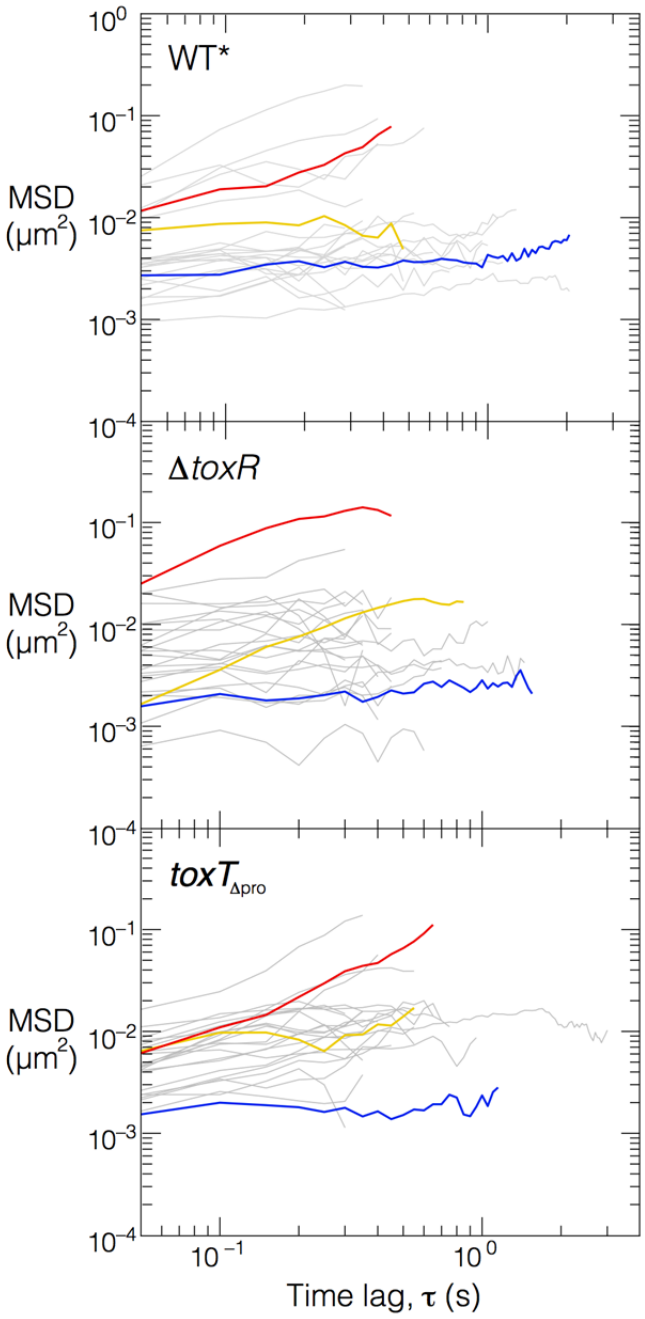

Fig. S2. Single-molecule MSD curves

MSD curves for representative single TcpP-PAmCherry molecules in WT* (top) Δ*toxR* (middle) and $toxT_{\Delta pro}$ (bottom) strains. The three colored curves (red, yellow and blue) in each plot correspond to the like-colored trajectories in Fig. 2B, 3B and 3D, respectively. Gray curves correspond to the additional white trajectories in Fig. 2B, 3B and 3D. All plots show time lag values up to two-thirds of the maximum time lag.

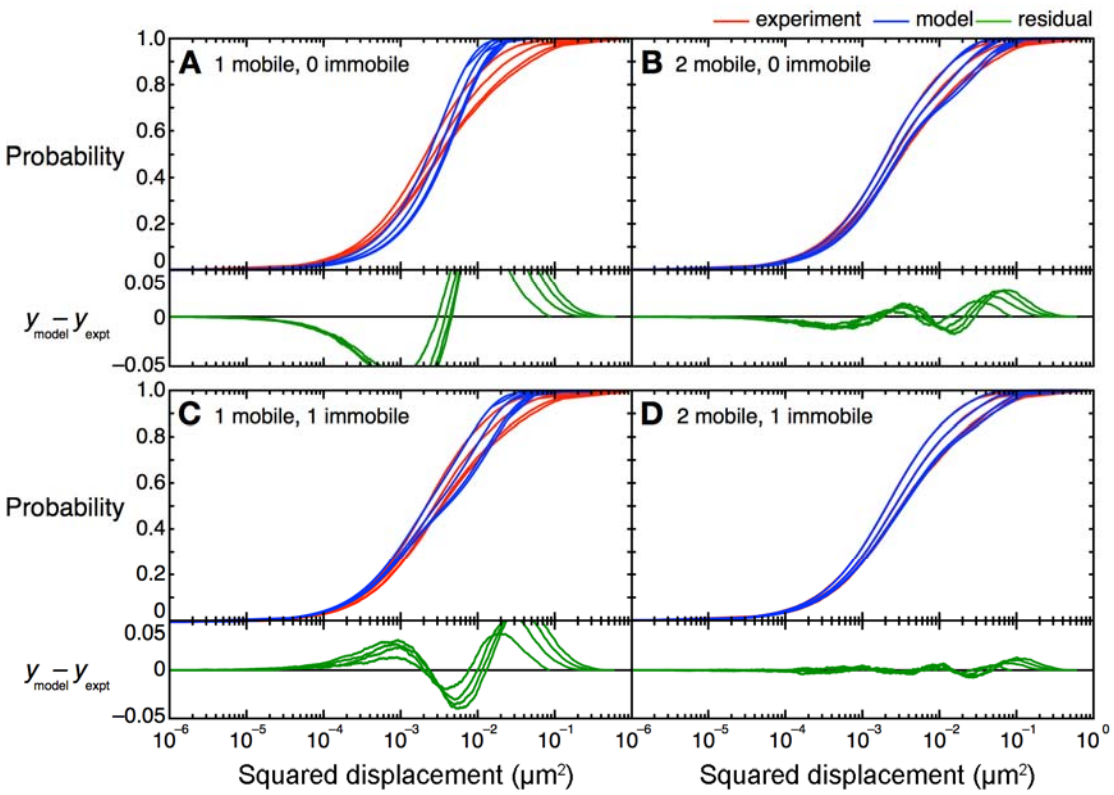

Fig. S3. CPD fits and residuals

A three-term model, with two mobile populations and one immobile population, described the WT* CPD data best (panel D); this corresponds to Fig. 2C in the main text. Models with fewer terms (panels A–C) fit poorly, as seen in the plots of their residuals (green curves). Fits to a model with an extra fit parameter (i.e., three mobile terms) identified one essentially immobile term, and yielded the same result as the two mobile terms plus one immobile term model. In each attempted model, only terms differing by an order of magnitude were considered unique.

Experimental data is shown in red and best fits for each of the given models are shown in blue. Curves for the first four time lags (50–200 ms) are plotted left to right. Residuals (i.e., the differences between each of the models and the experimental results) are shown in green.

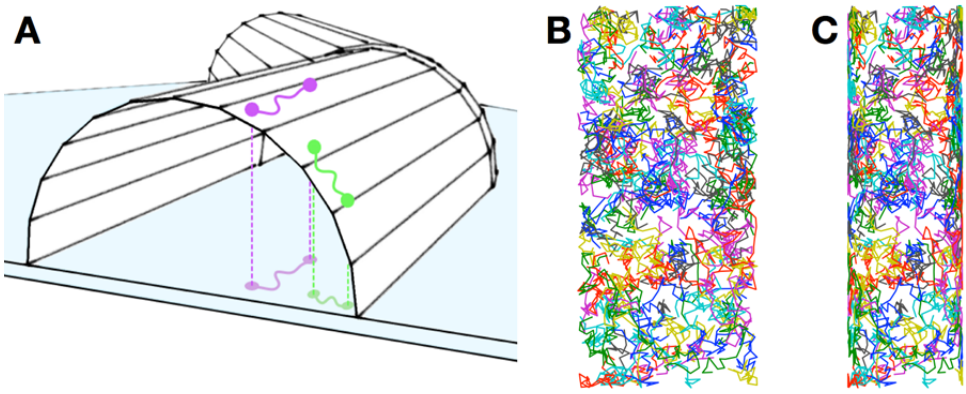

Fig. S4. 3D curved cell vs. 2D projection

A. The purple and green paths are the same length on the surface of the cell, but when projected onto the imaging plane (represented by the blue surface), the green path appears shorter than the purple path due to the curvature of the cell membrane.

B. 200 two-dimensional random walks on the surface of a cylinder.

C. The projection of the walks in B onto a simulated two-dimensional detector.

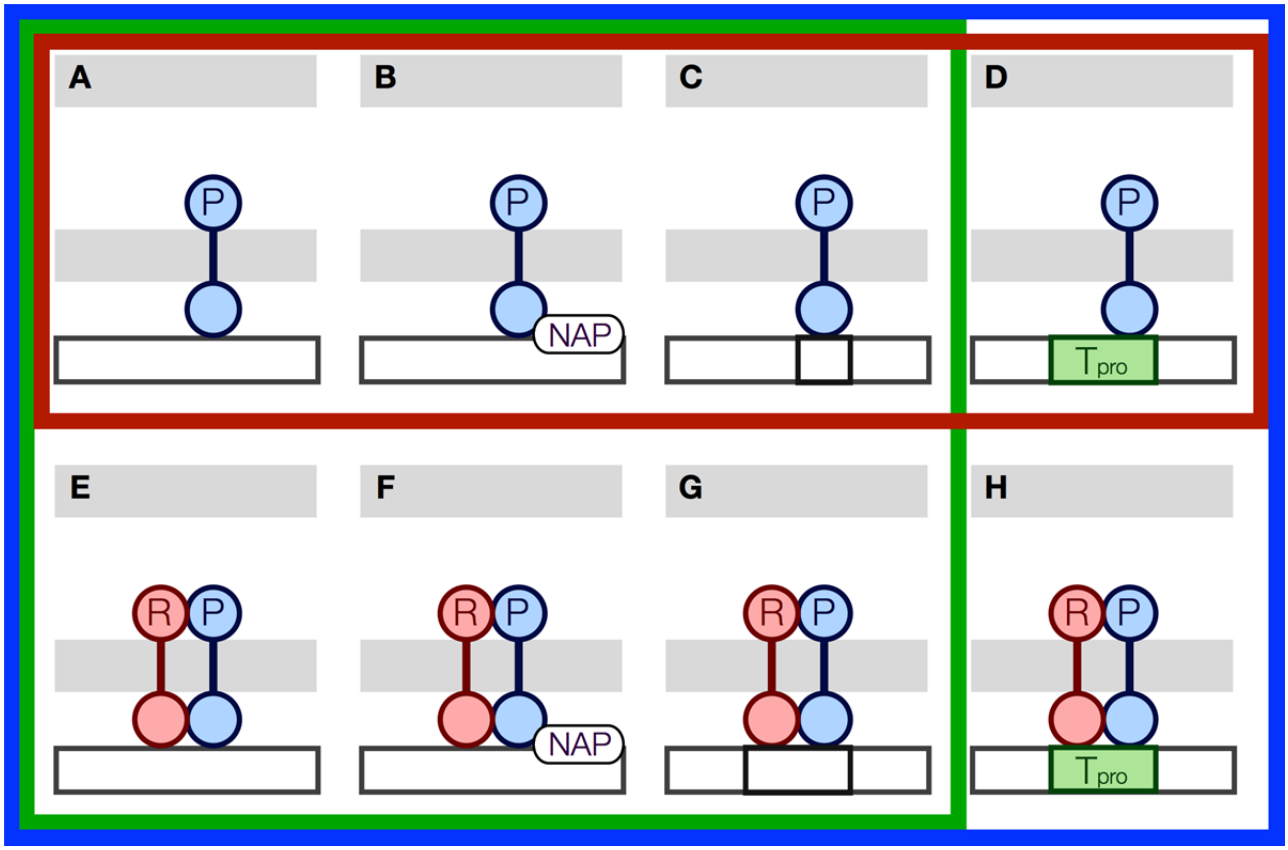

Fig. S5. Expected modes of TcpP motion

A. TcpP (P) moving along DNA

B. TcpP blocked by a nucleoid associated protein (NAP)

C. TcpP binding nonspecifically to DNA

D. TcpP bound specifically to the *toxT* promoter (T_{pro})

E–H. Modes A–D in the presence of ToxR (R).

Of the modes shown, only interactions A–F can occur in the Δ*toxR* mutant (red box), and only modes A–C, and E–G are possible in the $toxT_{\Delta pro}$ strain (green box). All eight modes can occur in the WT* strain (blue box). Additional modes of motion, such as freely diffusing TcpP and TcpP interacting with ToxR without binding DNA, are too fast to be captured by our imaging conditions (20 frames per second).

Supporting References

Kay B.A., Bopp C.A., and Wells J.G. (1994) Isolation and identification of *Vibrio cholerae* O1 from fecal specimens. In *Vibrio Cholerae* and Cholera: Molecular to Global Perspectives. Wachsmuth, I.K., Blake, P.A., and Olsvik, Ø (eds). Washington, DC: American Society for Microbiology Press, pp. 3-26.

Lommerse P.H.M., Blab G.A., Cognet L., Harms G.S., Snaar-Jagalska B., Spaink H.P., and Schmidt T. (2004) Single-molecule imaging of the H-Ras membrane-anchor reveals domains in the cytoplasmic leaflet of the cell membrane. *Biophys J* **86:** 609-616.

Qian H., Sheetz M.P., and Elson E.L. (1991) Single particle tracking. analysis of diffusion and flow in two-dimensional systems. *Biophys J* **60:** 910-921.

Sonnleitner A., Schütz G.J., and Schmidt T. (1999) Free Brownian motion of individual lipid molecules in biomembranes. *Biophys J* **77:** 2638-2642.

van den Wildenberg, S.M.J.L., Bollen Y.J.M., and Peterman E.J.G. (2011) How to quantify protein diffusion in the bacterial membrane. *Biopolymers* **95:** 312-321.